Topographic comparisons of uplift features on Venus and Earth: Implications for Venus tectonics

Paul R. Stoddard [a,*], Donna M. Jurdy [b]

[a] Dept. of Geology and Environmental Geosciences, Northern Illinois University, DeKalb, IL 60115-2854, United States
[b] Dept. of Earth and Planetary Sciences, Northwestern University, Evanston, IL 60208-2150, United States

ARTICLE INFO

ABSTRACT

Venus and Earth display different hypsography. We use topographic profiles to search for well-understood terrestrial analogs to venusian features. Specifically, by using cross-correlation, we correlate average profiles for terrestrial rifts (slow and fast, "ultra-slow," incipient and inactive) and also hotspots (oceanic and continental) with those for venusian chasmata and regiones, to draw inferences as to the processes responsible for shaping Venus' surface. Correlations tend to improve with faster spreading rates; Venus' correlations rank considerably lower than terrestrial ones, suggesting that if chasmata are analogous to terrestrial spreading centers, then spreading on Venus barely attains ultra-slow rates. Individual features' normalized average profiles are correlated with profiles of other such features to establish the degree of similarity, which in turn allows for the construction of a covariance matrix. Principal component analysis of this covariance matrix shows that Yellowstone more strongly resembles Atla, Beta and W. Eistla regiones than it does the terrestrial oceanic hotspots, and that venusian chasmata, especially Ganis, most closely resemble the ultra-slow spreading Arctic ridge.

© 2011 Elsevier Inc. All rights reserved.

1. Introduction

Earth and Venus have many similar features, yet their tectonic histories are quite different. Like the Earth, Venus has a global rift system, which has been cited as evidence of tectonic activity, despite the apparent lack of Earth-style plate tectonics. Both systems are marked by large ridges, usually with central grabens. On Earth, the topography of the rifts can be modeled well by a cooling half-space and the spreading of two divergent plates. The origin of the topographic signature on Venus, however, remains enigmatic. Even with 1978 Pioneer mission altimetry, the absence of topographic features analogous to ocean ridges was apparent (Kaula and Phillips, 1981). These data enabled Schaber (1982) to identify a global system of extensional features on Venus as evidence of tectonic activity. He attributed the extension to upwelling processes, such as at Earth's continental rift zones, and noted that the global scope of these extension zones, similar in scale to Earth's mid-ocean ridges, could be fit by great circle arcs.

Venus' rift zones (termed "chasmata") extend 1000s of kilometers. This chasma system, as imaged by Magellan, can be fit with great circles measuring 54,464 km (Jurdy and Stefanick, 1999). When corrected for the smaller size of Venus, this nearly matches the 59,200-km total length of the spreading ridges determined for Earth (Parsons, 1981). Venus and Earth also both have large regions of apparent upwelling – hotspots on Earth, and regiones on Venus (Stofan and Smrekar, 2005). These are marked by broad topographic and geoid highs as well as evidence of volcanic activity.

In this paper, we use topographic profiles to look for well-understood terrestrial analogs to venusian features. Specifically, we cross correlate average profiles for terrestrial rifts, slow and fast, as well as "ultra-slow", incipient and extinct, and hotspots (oceanic and continental) with those for a variety of venusian chasmata and regiones. Comparing the profiles, we then draw inferences as to the processes responsible for shaping Venus' surface.

1.1. Hypsography

Hypsographic curves represent the relative area/distribution of a body's topography. Even a preliminary glance at the hypsographs for Earth, Venus, the Moon, and Mars (Fig. 1) shows a large variety of distributions. We note the well-known bimodal distribution of topography for Earth, reflecting the topographic dichotomy of continents and ocean basins, a consequence of plate tectonic processes. At the other end of the spectrum, we see Venus with a near-Gaussian distribution, perhaps signifying one dominant resurfacing process – volcanism. The Moon looks similar to Venus in its hypsographic distribution, while Mars more closely resembles the Earth. Each of these bodies has its unique surface-shaping processes and history recorded in its hypsography.

---

* Corresponding author.
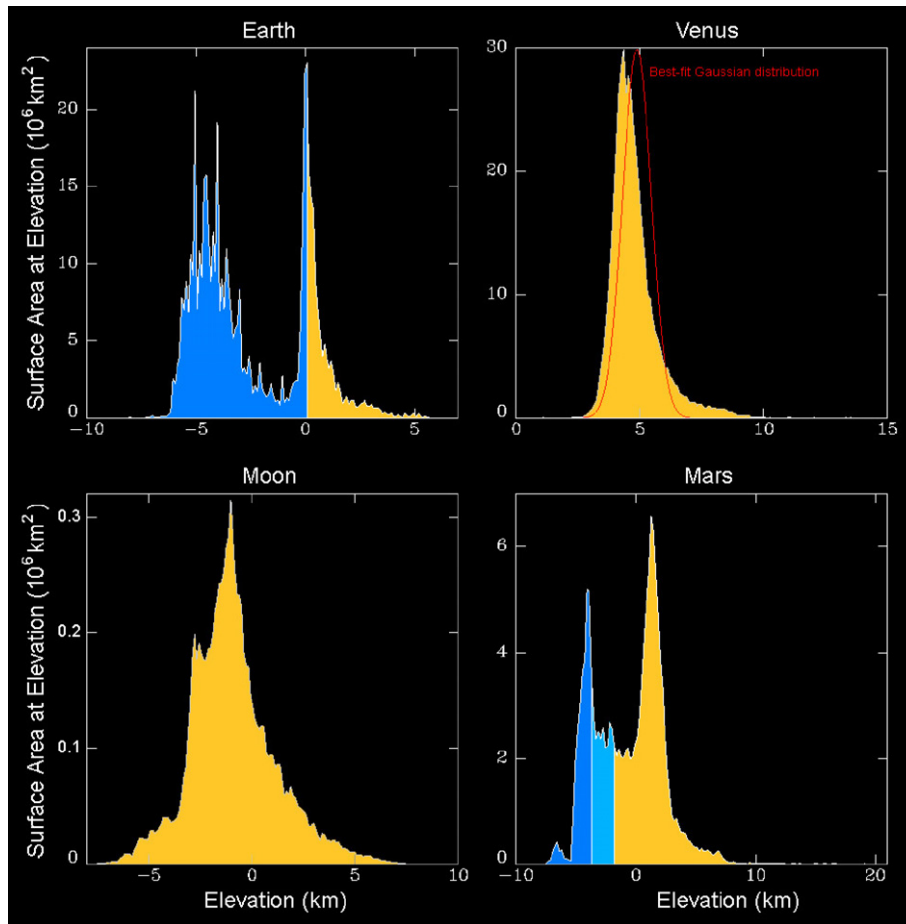E-mail address: prs@geol.niu.edu (P.R. Stoddard).

Fig. 1. Hypsographs for Venus, Earth, Moon, and Mars. A best-fit Gaussian curve (red) is shown for Venus. Blue regions represent below sea-level portions of the terrestrial curve, and portions below two sea levels proposed for Mars. The bimodal distribution for Earth is attributable to differing densities of basalt (seafloor) and granite (continents). Venus' distribution is distinctly unimodal, implying only one dominant surface rock type. (For interpretation of the references to color in this figure legend, the reader is referred to the web version of this article.)

The underlying importance of Earth's bimodal hypsography was noted early last century. In 1929, Wegener (1966, p. 37) presciently observed: "In the whole of geophysics there is hardly another law of such clarity and reliability as this – that there are two preferential levels for the world's surface which occur in alternation side by side, and are represented by the continents and ocean floors, respectively. It is therefore very surprising that scarcely anyone has tried to explain this law, which has, after all, been well known for some time... In this way we have achieved for the first time a plausible explanation..." He explained the bimodal elevation distribution with the fundamental difference in continental and oceanic crust, this supporting his theory of Continental Drift. As Wegener realized, topographic data hold clues for understanding the history of a planet's surface. Earth's hypsometric curve has more recently been explained by plate tectonics, and shows some second-order effects, such as the peaks in the seafloor portion, which may reflect periods of fast spreading.

Unlike Earth, Venus does not appear to have plate tectonics. Comparison of the hypsographs for the two planets (Fig. 1) reflects major differences in the processes shaping their surfaces – Earth's bimodal distribution results from the two major rock types, granite and basalt, whereas Venus seems dominated by only one type of rock, presumably basalt. Of the terrestrial bodies, Venus displays the simplest hypsography, with 80% of its surface within 1 km elevation of the mean (Ford and Pettengill, 1992). The near-Gaussian distribution bears an overall similarity to the distribution of the continental portion of Earth's curve and the higher elevation portion of Mars' curve, and to a lesser degree, to the curves of the

Moon and Earth's oceans. This suggests that Venus's hypsography may represent the typical distribution of a one rock-type surface.

Mars may have seen two ancient sea-level stands (Parker et al., 1993). Both have signatures in the hypsograph (Fig. 1) with the lower stand much more pronounced, and indeed only the deeper sea-level stand is supported by MOLA evidence (Head et al., 1999). Although Mars' bimodal distribution is similar to that caused by Earth's plate tectonic processes, it has been attributed to offset of center of mass from center of figure (Smith and Zuber, 1996).

The Moon's hypsographic curve features a shoulder at about −3 km, perhaps due to volcanic infill of major basins. Another satellite, Saturn's Titan, unique in so many ways, displays a hypsometric curve with a negative tail (Lorenz et al., 2011). This could be the result of collapse on Titan's surface. Cassini's radar can image Titan's surface beneath the thick clouds and has revealed numerous dark circular features in the equatorial region. These may be related to methane–cryovolcanism, and have been interpreted as collapse features, or pits. For a portion of Cassini's equatorial swath, Adams and Jurdy (2011) identified 195 pits with diameters between 1 and 6 km (3–17 pixels), and from the Poisson distribution they inferred the probable number of additional pits in the region below the resolution of 3 pixels. They conclude that in total, pits could account for 0.5% of the area, thus contributing noticeably to Titan's hypsography.

The remaining unexplored terrestrial body, Mercury, is scheduled to be fully mapped by MESSENGER, following its March, 2011 orbit insertion. Until then, we can only guess about the char-

acter of its hypsometry. Based on a superficial resemblance with the Moon in terms of cratering and suspected volcanic provinces, we might anticipate a hypsometry for Mercury similar to that of the Moon.

2. Procedure

This study utilizes Magellan topography data for Venus and ETOP05 for Earth. The Magellan mission, 1990–1994, provided nearly full coverage of Venus. The altimetry footprint was dependent on direction and latitude, but generally ranged between 10 and 30 km, and the vertical resolution was typically 5–50 m. ETOP05 data vary in resolution, but the highest resolution data (oceans, USA, Europe, Japan, and Australia) have horizontal resolution of 5 min of latitude and longitude, and vertical resolution of 1 m (NOAA, 1988). Given the scale of the features being examined (100s of km), these resolutions are more than adequate.

Using these data, and techniques described more fully in Jurdy and Stoddard (2007), we analyze profiles for the Africa/South America portion of the slow-spreading Mid-Atlantic Ridge and the Pacific/Nazca portion of the fast-spreading East Pacific Rise for comparison with profiles for Ganis Chasma on Atla Regio, and Devana Chasma which extends from Beta Regio to Phoebe Regio (Price and Suppe, 1995). These rifts are among the most recently active on Venus (Basilevsky and Head, 2002) with profuse volcanism as documented by the nature of cratering.

For ridge features, we take profiles perpendicular to the ridge trend every half-degree or so. For uplift features, we take 36 radial profiles through the center of the feature at 10° intervals. Note that there are actually only 18 independent radial profiles, as those separated by 180° are mirror images. Profiles in this study were analyzed in sets, from 800 to 2400 km long. Profiles used for Earth are shown in Fig. 2a, those for Venus in Fig. 2b.

For each feature, we average all profiles, and then cross correlate the individual profiles with the average. Each profile is shifted to find the maximum correlation with the average. Finally, we cross correlate the average profiles of each feature with each other to arrive at our correlation percentages. Fig. 3 shows examples of

rifts from Earth and Venus. Terrestrial and venusian uplift examples are shown in Fig. 4.

We examine a range of terrestrial spreading centers: fast (East Pacific Rise), slow (Mid-Atlantic Ridge), ultra-slow (Arctic), incipient (East Africa Rift), and extinct (Labrador Rift), and compare these to several chasmata on Venus (Devana, Ganis, Juno, Parga, Kuanja, and an isolated, unnamed one, here called "Lonely" positioned in the area 40–65°S, 45°W–40°E). For upwelling regions, we consider the oceanic Hawaii, Reunion, and Iceland hotspots and Yellowstone, a hotspot beneath a continent on Earth. On Venus, broad topographic and geoid highs, called regions, have been characterized by Stofan and Smrekar (2005). Venus has approximately a dozen, and we examine Atla, Beta, and W. Eistla regiones. Atla and Beta are widely thought to be the most likely to be currently or recently active (Basilevsky and Head, 2002; Matias and Jurdy, 2005; Jurdy and Stoddard, 2007); also, we include W. Eistla for comparison with these two.

3. Results

We compare terrestrial and venusian features using several techniques: cross-correlation of feature profiles, principal component analysis of the profiles, and Fourier analysis of the topography.

3.1. Correlations

Not surprisingly, the most closely related features (the MAR and EPR spreading rifts on Earth; Atla, Beta, and W. Eistla regiones on Venus) have the highest cross-correlations. Next best are the correlations between the venusian and terrestrial rifts, and the correlation between the Yellowstone hotspot and Atla and Beta regiones. Yellowstone correlated only moderately well with the Earth's oceanic hotspots and Venus' regio, W. Eistla. Correlations with Iceland are probably somewhat poorer than might be expected for a hotspot, due to the domination of the Mid-Atlantic Ridge and Iceland's proximity to Greenland, which affects the topography of some profiles. This lowers the overall correlation.
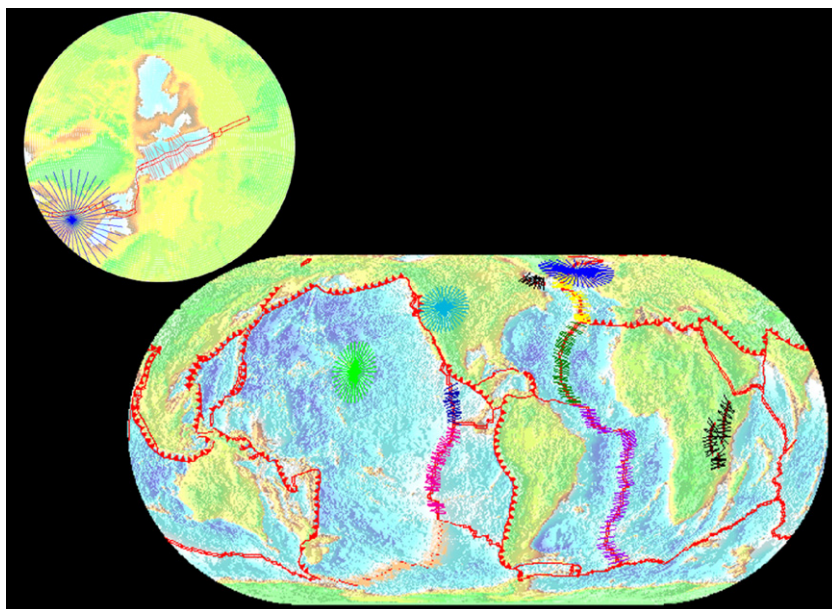

Fig. 2a. Earth profiles for uplifts, ridges and locations of rifting, current incipient and extinct, with bathymetry (warm colors high, cool colors low). Profiles are taken perpendicular to the ridge trend every half-degree; for uplift features, 36 radial profiles are taken through the center. Rifts: yellow, N. America/Eurasia; green, N. America/ Africa; purple Africa/S. America; dark blue, Pacific/Cocos; pink, Nazca/Pacific; tan, Pacific/Antarctica, black, E. African. Rift; dark gray, Labrador; orange, Arctic (inset). Uplifts: blue, Iceland; teal, Yellowstone; green, Hawaii.
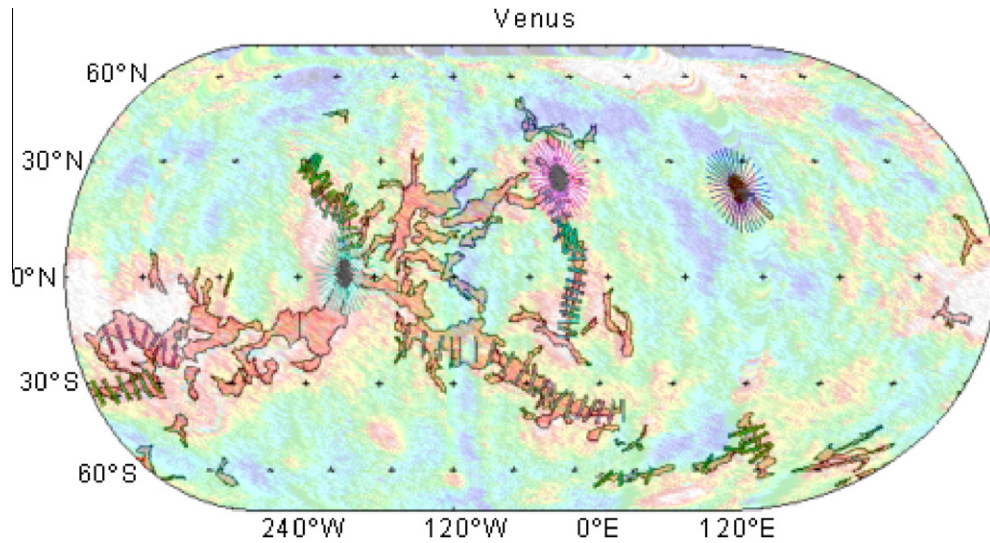
Fig. 2b. Venusian profiles for regiones and chasmata, with bathymetry (color scheme as for Earth). Rift regions are shown as outlined pink areas. Regiones: teal, Atla; pink, Beta; dark blue, W. Eistla. Chasmata: aqua (trending S from Beta), Devana; green (trending NW from Atla), Ganis; green-gray (trending SE from Atla), Parga; green (30°S, 250°W), Juno; pink (12°S, 260°W).
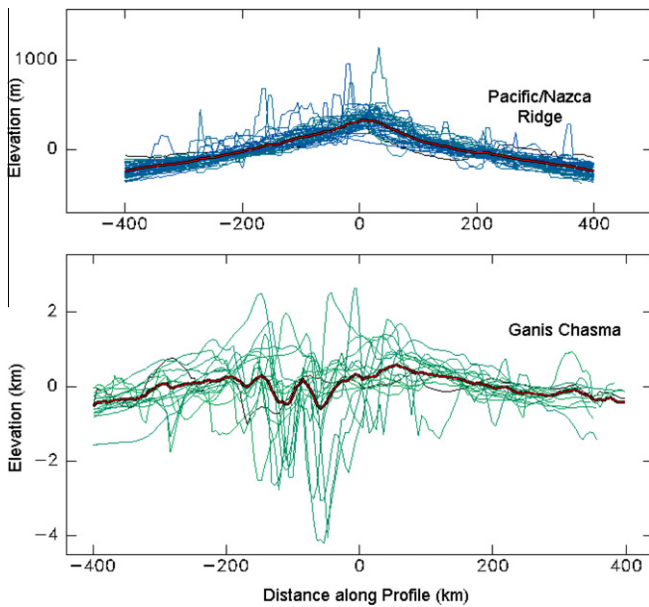

Fig. 3. Examples of correlations for Earth (top) and Venus (bottom). For Earth, individual profile lines taken along the ridge are blue. For Venus, green lines are individual profile lines taken along the chasma. For both, dark lines are the averages of the individual profiles. (For interpretation of the references to color in this figure legend, the reader is referred to the web version of this article.)

In Fig. 5a, we display the correlations of individual profiles for terrestrial spreading centers with the average profile. For each section of the ridge corresponding to a plate pair, the individual profiles are correlated with the mean to determine a correlation coefficient. The spreading rates are indicated for each section. Correlations tend to improve with faster spreading rates (it has long been observed that fast-spreading ridges are more uniform in shape); however, correlations are reduced near triple junctions. The Arctic profiles have very poor correlations, perhaps reflecting the ultra-slow spreading of the Arctic ridge. In a study that did not include more recent data from the Arctic, Stoddard (1992) noted an apparent "lower speed limit" for spreading rates. The anomalously poor correlation of the Arctic profiles, coupled with the anomalously slow rates, indicates that spreading processes in
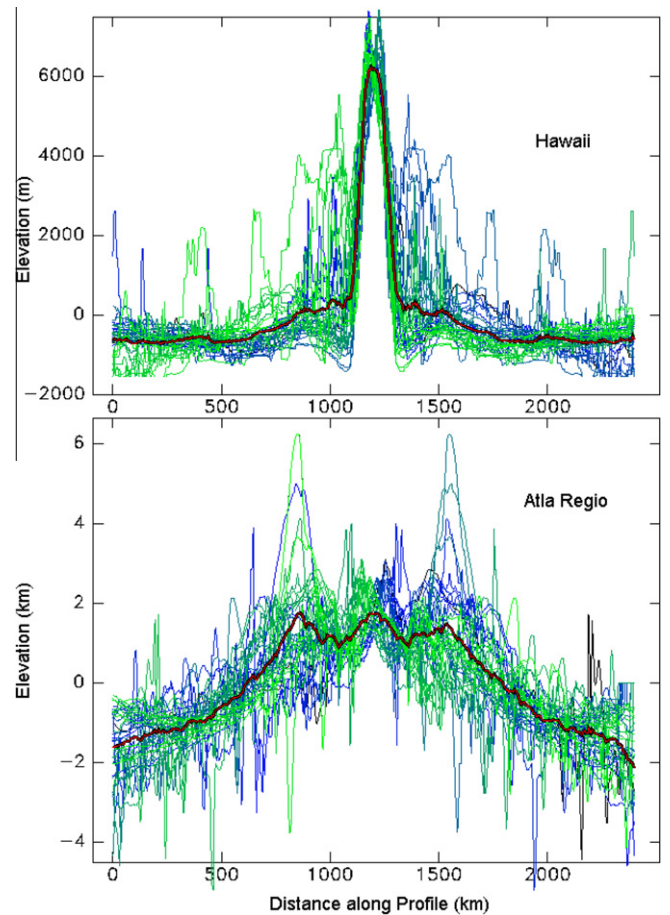

Fig. 4. Examples of correlations for upwelling regions on Earth (top) and Venus (bottom). Blue/green lines are individual profiles color-coded by azimuth. (N.B. Since lines for azimuth 0° and 180°, e.g., are mirror images of each other, blue lines will have a green mirror image on these composite plots.) (For interpretation of the references to color in this figure legend, the reader is referred to the web version of this article.)

the Arctic may fundamentally differ from other ridges. Dick et al. (2003) identify the Arctic as an "ultra-slow" spreading ridge. These
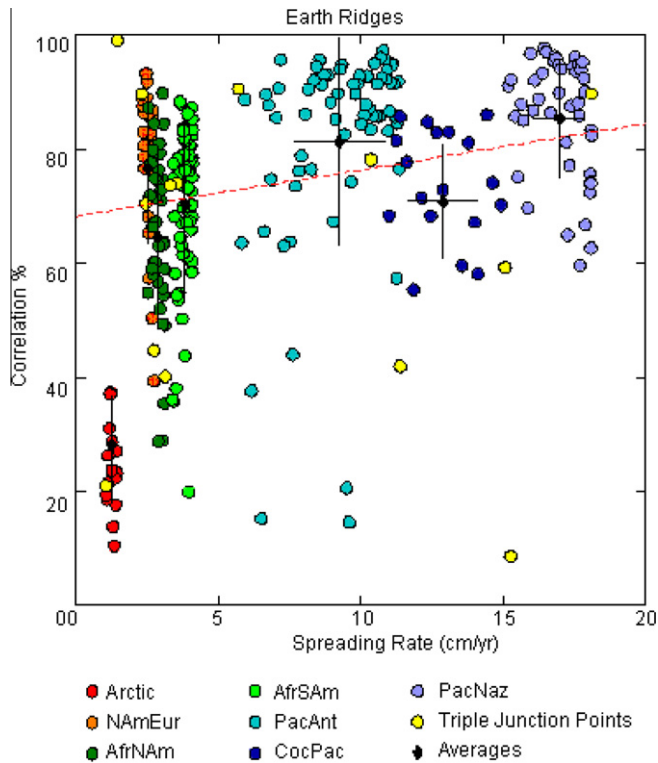
Fig. 5a. Terrestrial profile correlation percents as a function of spreading rate. Percents are the cross-correlations of individual profiles with the average for that plate pair, divided by the autocorrelation of the average profile. Points are color coded by plate pair. Red: N. America/Eurasia (Arctic ocean); orange: N. America/Eurasia (Mid-Atlantic Ridge); dark green: Africa/N. America; light green: Africa/S. America; teal, Pacific/Antarctica; blue: Cocos/Pacific; purple, Pacific/Nazca. Averages (by plate pair) of correlation percent and spreading rate are indicated by black diamonds and uncertainty bars (1 s.d.). Profiles near triple junction points are highlighted (yellow), as their topography may be influenced by their proximity to the triple junction.

Fig. 5b. Venusian profile correlation percents as a function of distance along the chasma. Percents are the cross-correlations of individual profiles with the average for that chasma, divided by the autocorrelation of the average profile. Distance was chosen as a proxy for spreading rate, since if these were spreading rifts as on Earth, the rate would vary as a function of distance along the rift from the Euler pole. Points are color coded by chasma.

ridges with intermittent volcanism, full-spreading rates less than 20 mm/yr and generally lacking transform faults are considered an end-member in the terrestrial seafloor-spreading continuum. Ultra-slow spreading centers, like the Arctic, may represent a distinct class of ridges (Dick et al., 2003).

A relationship between spreading rate and correlation is suggested by the analysis of terrestrial rifts, with faster spreading having higher correlations. In other words, faster ridges are more uniform in their morphology. Venus' correlations (Fig. 5b) rank considerably lower than the terrestrial ones plotted with their corresponding spreading rates. Extrapolating the correlation/spreading rate trend to Venus therefore indicates that if chasmata are analogous to terrestrial spreading centers, spreading rates on Venus barely attain the ultra-slow spreading level (less than 12 mm/yr) of the Arctic.

Comparisons were made between features of presumed like and unlike origins. In general, for the longer, 1200-km profiles, the correlations among Earth's rifts and among Venus' uplifts were the highest. Earth's rifts actually correlated better with Venus' uplifts (68%) than with terrestrial uplifts (50%). Venusian rifts and uplifts correlated at about the same level (48%) as their terrestrial counterparts. Looking at individual correlations, it is interesting to note that Yellowstone correlates more closely with the Atla and Beta regions on Venus than it does with the Hawaii or Iceland hotspots.

Using shorter profile lengths, Stoddard and Jurdy (2005) found that Atla and Beta most closely correlated to Earth's spreading rifts, in agreement with Stofan and Smrekar's (2005) ranking of these two regions as the most rift-dominated on Venus. The difference
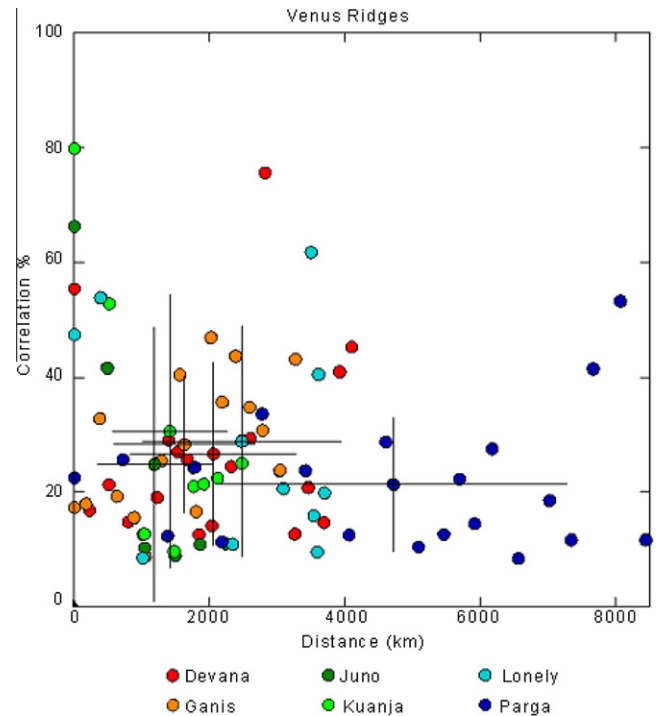
between the long- and short-profile correlations suggests that the topography of the more local constructs of the regiones is dominated by rifting, whereas the longer-wavelength profiles reflect the larger-area upwelling processes. Further comparisons using the shorter, 400-km, profiles used in the analysis presented here show that the Arctic, East African, and Labrador rifts correlate poorly compared with the more typical spreading centers. Of these three, the E.A.R. compares the best. Terrestrial uplifts correlate at a relatively high 70% with each other, but at only 30% with those from Venus. Among the venusian uplifts, the correlation percent is only 13%.

Comparison was made between the correlations among the long- and short-profile sets. For each feature pair, the correlation percent for the 1200-km profiles is divided by that for the 400-km profiles. In virtually every case, the terrestrial correlations are stronger for the shorter profiles, while the venusian are stronger for the longer profiles.

Average profiles for the 15 rifts for Earth and Venus are shown in Fig. 6, ordered from the top as a function of spreading rate (for terrestrial rifts). In addition, Fig. 6 (left) compares terrestrial hotspot profiles with regiones on Venus. Considerable difference of opinion rages on the choice and validity of individual hotspots (e.g. Foulger and Jurdy, 2007). Here, we have selected Hawaii, Reunion and Iceland, features all characterized as "Type 1" by Courtillot et al. (2003) as being the manifestations of the deepest, primary plumes; Yellowstone, selected as a representative for a continental hotspot, does not have primary plume status.

3.2. Principal component analysis

A quantitative comparison of topographic features on Venus and Earth is undertaken through principal component analysis
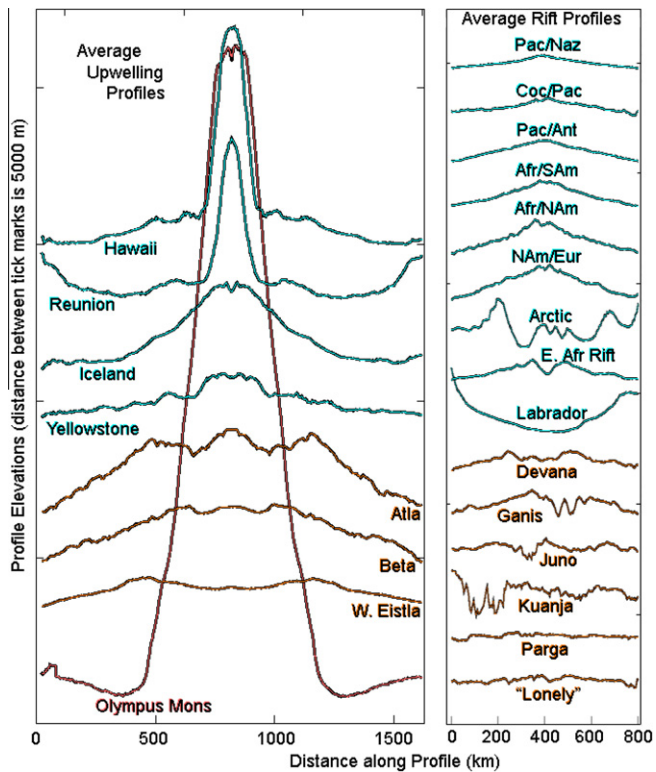
Fig. 6. Comparison of average profiles for all features analyzed in this study. Aqua – terrestrial features. Orange – venusian features. Red – Olympus Mons (Mars). (For interpretation of the references to color in this figure legend, the reader is referred to the web version of this article.)

(PCA). First, the correlation coefficients for pairs of features are determined from their normalized average topographic profiles. These correlation coefficients are then arranged in a covariance matrix, which is diagonalized to find the eigenvalues, or principal components. The principal components assess the degree of similarity and variability of the shapes of the average profiles. PCA thus offers an independent and objective mode of comparison (Lay, 2006). The appendix gives the theory for PCA.

Next we pose tectonic questions about uplift features on Venus and Earth, and then address these with PCA.

3.2.1. Are Earth's hotspots an analog for circular uplifts on Venus, the regiones?

To address this question, and as a step-by-step example of (PCA), we analyze these features. We start with their correlations, to determine the principal components of the covariance matrix by diagonalization. Our goal is the quantitative comparison of well-understood terrestrial uplift features, ranging from the generally-accepted archetype of an oceanic hotspot, Hawaii, and its Indian Ocean counterpart, Reunion, to Iceland, a hotspot positioned on the North Atlantic spreading center, to Yellowstone, one beneath the North American continent. However, as noted earlier, any choice of "typical" hotspots on Earth remains controversial. For Venus regiones we use Atla, Beta and W. Eistla. Atla and Beta have been classified by Stofan and Smrekar (2005) as "rift-dominated," unlike W. Eistla, which is representative of the "volcano-dominated" regiones.

In determining the principal components for these seven features, first the average profiles (Fig. 6) are normalized. By pairs, the features are correlated and a covariance matrix constructed, shown in upper part of Table 1. Diagonalizing this 7×7 matrix, we find the seven eigenvectors, or principal components. The prin-

cipal components, with corresponding weights, for each of the seven uplift features are given in the lower portion of Table 1, and illustrated in Fig. 7. The trace of the covariance matrix sums to 700, so the first principal component with a value of 398.5 alone accounts for 56.9% of the variance of the topographic profiles. The first three components (values 398.5, 168.5, 100.36) together account for over 95% the shape of the profiles. Thus, the topographic profiles of the seven uplifts on Venus and Earth can be very nearly described with just three independent components. The profiles corresponding to each of these components can be constructed from the weights and are shown in Fig. 8. The remaining four components, as a group, contribute less than 5% of the variance and are insignificant in constructing the profiles.

We can draw a number of conclusions from the principal component analysis of these circular features. The first, the largest component, corresponds to an uplift. This component is positive for all seven features, but here we see that the 40+% levels for Atla and Beta more resemble Iceland and Yellowstone than the ocean hotpots, Hawaii and Reunion. The second component, on the other hand, differs by planet: negative for the four terrestrial hotspots, but positive for the venusian regions. Indeed, the profile for this component (Fig. 8) characterizes how the topographic profiles of uplifts on Earth and Venus differ. The third component, most strongly represented for W. Eistla's profile, makes variable, but small, contributions for the other features.

3.2.2. Which of Earth's spreading centers most resembles the chasmata of Venus?

Here we use PCA to compare the profiles of 8 terrestrial spreading centers to four venusian chasmata. The terrestrial rifts cover the various stages and full range of spreading, from the fastest-spreading Pacific–Nazca rise, to the more moderate-spreading in the Atlantic represented by the Africa–North America and North America–Europe ridges, to the ultra-slow spreading Arctic Ocean. The East African Rift represents incipient seafloor spreading and the Labrador Sea, extinct, or inactive, seafloor spreading. For Venus, Devana, Ganis, Parga and Juno chasmata were chosen for comparison. For this example, the 12×12 covariance matrix has a trace of 1200, shown in the upper portion of Table 2. Diagonalizing this matrix we find the first three principal components (Table 2) of 638.5, 155.4, and 90.3, which account for 73.8% of the variance. The first component is positive for all 12 features: ~0.4 for the actively spreading terrestrial ridges, whereas the ultra-slow Arctic is only 0.06 and the incipient East African rift comes closer to the active ridges at 0.3. The Venus chasmata all have a smaller first component. Again, the second principal component differentiates between planets: terrestrial spreading centers have negative values, whereas the Arctic is strongly positive at 0.6 and the Venus chasmata are also positive, as is the Labrador Sea. Thus, we conclude that topographic profiles of Venus chasmata most closely resemble the Arctic, characterized as ultra-slow.

3.2.3. How do Venus circular uplift features compare with terrestrial rifts?

To compare these features we construct an 11×11 covariance matrix including the same three regions from the first analysis (Atla, Beta and W. Eistla) with the eight terrestrial spreading centers for a range of rates and states discussed above. As with the other examples, the largest principal component is positive for all 11 features, with the active spreading ridges having very similar values. The East African Rift does not quite reach the level of the active oceanic rifts, and Labrador and the Arctic have values that are lower still, as do the venusian regions. Here we see the same pattern for the second principal component: the normal terrestrial spreading centers have negative values, whereas the Arctic and Labrador are positive, as are the regions of Venus. As with the pre-

Table 1
Top: Correlation matrix for 800-km long average profiles of terrestrial and venusian uplift features. *Bottom*: Principal component matrix. The strongest three components are highlighted.

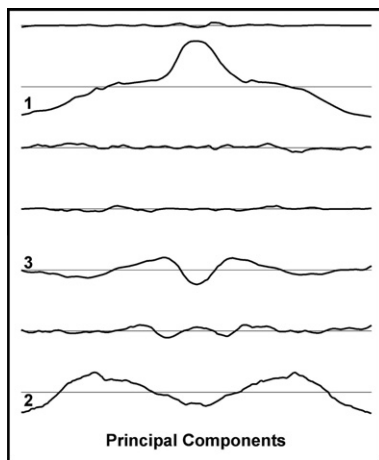|	Hawaii	Reunion	Iceland	Y'stone	Atla	Beta	W. Eistla
Hawaii	100	85	62	68	32	29	17
Reunion	85	100	39	41	9	11	25
Iceland	62	39	100	94	52	65	14
Yellowstone	68	41	94	100	60	66	15
Atla	26	7	43	49	100	89	77
Beta	24	9	53	54	89	100	63
W. Eistla	13	20	11	11	77	63	100
Principal component strength	**398.5**	**168.5**	4.8	16.78	10.52	**100.4**	0.53
Normalized PC	**0.57**	**0.241**	0.007	0.024	0.015	**0.143**	0.0008
Hawaii	**0.37**	−0.46	−0.46	0.54	0.16	**0.22**	0.28
Reunion	**0.27**	−0.49	0.36	−0.36	0.14	**0.53**	−0.37
Iceland	**0.43**	−0.17	−0.49	−0.45	−0.35	**−0.42**	−0.23
Yellowstone	**0.44**	−0.16	0.63	0.12	−0.23	**−0.38**	0.40
Atla	**0.41**	0.42	0.1	0.5	−0.13	**0.04**	−0.62
Beta	**0.42**	0.36	−0.04	−0.25	0.77	**−0.13**	0.14
W. Eistla	**0.28**	0.44	−0.1	−0.22	−0.41	**0.58**	0.41

Fig. 7. Principal components for covariance matrix in Table 1, comparing terrestrial (Hawaii, Reunion, Iceland, Yellowstone) and venusian (Atla, Beta, W. Eistla) uplift features. Each trace is a representative trace, the sum of which, appropriately weighted, will reproduce the original profile. Summing the top three components (labeled 1, 2, and 3) accounts for 95% of the shape of the profiles in this example.

vious analysis, the active terrestrial oceanic rifts tend to cluster together; they cannot be distinguished on the basis of this PCA. These values for the principal components are in Table 3.

3.3. Fourier analysis

Fourier analysis of the average topographic profiles is applied to further characterize the topographic profiles of Venus and Earth. The power spectra of 22 average topographic profiles for Earth (13) and Venus (9) are found using Fourier analysis. As a group, the terrestrial profiles can be fit quite well with five or six Fourier components: Just three components are needed to fit active, spreading ridges at more than the 98% level: these include the Pacific–Nazca, Cocos–Pacific and Pacific–Antarctic spreading centers, as well as the entire Mid-Atlantic Ridge for the various plate pairs, and even the extinct Labrador ridge. However, the ultra-slow Arctic spreading center requires 11 components for the same level of fit, as coincidentally does the incipient East African Rift system. Venusian chasmata profiles would typically require more than 15 components to achieve the 98% level of fit, with the exception of only Devana Chasm. This is reflected in the power spectra computed from the autocorrelation: Venus' spectra are noticeably flatter than the spectra for Earth features.

Two rifts are compared in Fig. 7: Earth's Pacific–Nazca ridge with Venus' Ganis Chasma. The Pacific–Nazca plate boundary currently ranks as the fastest spreading plate boundary, with a full spreading rate of nearly 20 cm/yr (Fig. 5). Ganis Chasma lies in the BAT region, extending northwest from Atla Regio. Based on extensive crater modification (Matias and Jurdy, 2005) as well as the dip of craters away from Atla's peak, we assess this regio to be currently active (Jurdy and Stoddard, 2007). Thus, Ganis was chosen for display and comparison with an active terrestrial rift.

Uplifts for the two planets are compared in Fig. 9. Fourier analysis of Earth's hotspots, Yellowstone and Hawaii, fits both at the 99% level with 9 components; however, even with 15 components Venus' Atla Regio cannot be fit as well.

In general, faster-spreading features can be fit with lower wavenumbers. Venus features require considerably more components for the same level of fit. The Arctic spreading center most resembles Venus features in the Fourier decomposition. These results are in general agreement with the analysis of Venus' topography by Kucinskas et al. (1992); they established a fractal dimension for Tinatin Planitia and Ovda Regio topography that differs from similar analyses for Earth (c.f. Fig. 14.2, Feder, 1988; Huang and Turcotte, 1989).

4. Discussion

We compare topographic features on Venus and Earth to give insight into large-scale uplift features on Venus, regiones and chasmata, looking for better-understood terrestrial analogs. Topographic profiles are determined for a number of Earth's hotspots and spreading centers, ranging from the fastest spreading to ultra-slow, and including incipient and extinct spreading axes. Similarly for Venus, profiles are determined for regiones, both rift- and volcano-dominated, as well as a variety of chasmata. Earth's spreading centers, analyzed by plate pair, yield average profiles that correlate at a high level with individual profiles. Venus' chasmata, however, have topographic profiles that show considerably more variation, as evident in their power spectra. On Earth, it appears that fast-spreading ridges have a higher degree of correlation with each other than do slow-spreading ridges. The ultra-slow Arctic ridge falls below this trend, as do Venus' chasmata. On the basis of this correlation with average profiles, we determine that if the chasmata are indeed analogous to terrestrial spreading centers, they spread at rates corresponding to the ultra-slow Arctic rift, estimated as less than 20 mm/yr.

We find that Earth's plume-related uplifts, Iceland and Hawaii, each have significant radial symmetry, and thus strongly correlate
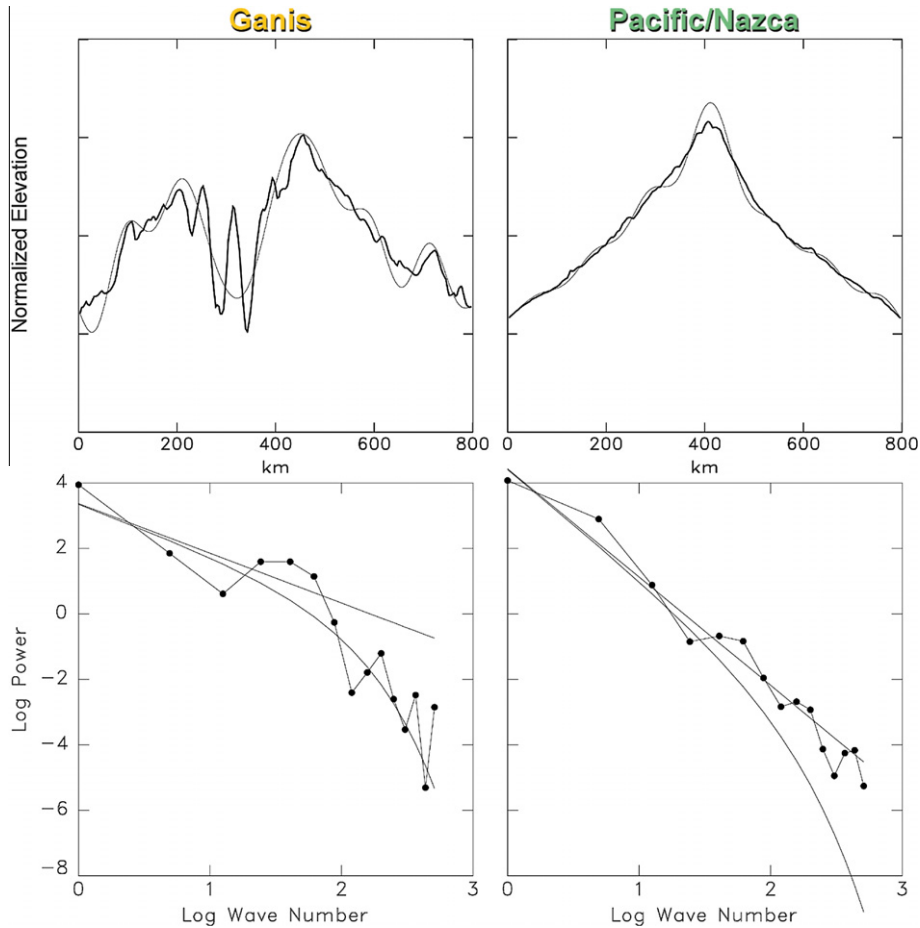
Fig. 8. (Top) Fourier analysis and power spectra comparing an average profile for a terrestrial spreading center (Pac/Naz) with that of a venusian rift (Ganis). Darker curve represents the average profile; the lighter curve, the Fourier fit using 15 components. (Bottom) Power spectra for the Fourier fit shown above, showing the relative contribution of the 15 components. Straight line shows a linear fit using only the first five wave numbers, and the curve represents the best fitting curve falling off with increasing wave number.

Table 2
Principal components for 800-km long average profiles of terrestrial and venusian rifts. (N.B: only the top four components are shown.)

Principal component strength	638.48	155.44	90.26	91.57
PA-AN	0.39	−0.11	−0.12	0.04
PA-NZ	0.38	−0.12	−0.19	−0.03
AF-SA	0.38	−0.13	−0.15	0.01
AF-NA	0.38	−0.10	−0.17	−0.04
NA-EU	0.38	−0.12	−0.12	0.06
Arctic	0.10	0.60	−0.01	0.19
E. Afr. Rift	0.31	−0.03	0.32	0.27
Labrador	0.16	0.13	0.36	−0.77
Devana	0.22	0.12	0.71	0.38
Ganis	0.18	0.34	0.12	−0.36
Parga	0.25	0.13	−0.13	−0.09
Juno	0.05	0.64	−0.35	0.13

Table 3
Top three principal components for comparison between 800-km long average profiles of terrestrial rifts and venusian uplifts.

Principal component strength	638.23	119.8	96.15
Atla	0.06	0.63	0.40
Beta	0.14	0.36	−0.66
W. Eistla	0.34	0.00	−0.11
PA-AN	0.39	−0.10	−0.01
PA-NZ	0.38	−0.08	0.04
AF-SA	0.39	−0.09	0.05
AF-NA	0.38	−0.09	0.03
NA-EU	0.39	−0.10	−0.02
Arctic	0.09	0.53	−0.37
E. Afr. Rift	0.29	−0.07	0.09
Labrador	0.15	0.39	0.49

with their average profile. Venus' Beta Regio, with lower topography, and the more active Atla Regio both display significant radial asymmetry, thus low correlation with the mean profile. Using covariance matrices constructed from the correlations of pairs of features, and employing principal component analysis of the covariance matrix, we establish that Yellowstone more strongly resembles Venus' regiones, Atla, Beta and W. Eistla, than it does Earth's oceanic hotspots. Perhaps this is a consequence of Venus' thicker lithosphere, so that the uplift of the regiones most resembles that of the Yellowstone plume beneath the North American continent. Future work would include an analysis of the effect of the length of the profiles.

A corresponding principal component analysis for rifts on the two planets also finds that Venus' chasmata most closely resemble the topography of the ultra-slow spreading Arctic Ocean. On the other hand, active terrestrial spreading centers, whether fast or slow, display little difference between them. In a separate analysis, Venus' regiones are compared with terrestrial rifts. Again, we find the strongest similarity with the Arctic. Only four Venus chasmata were considered in our analysis. Crustal thickness may play an important role in the development and response of chasmata. In detailed mapping of chasmata, Bleamaster and Hansen (2004) find that associated volcanic features, coronae, only develop for those chasmata in regions with lithospheric thickness less than 20 km
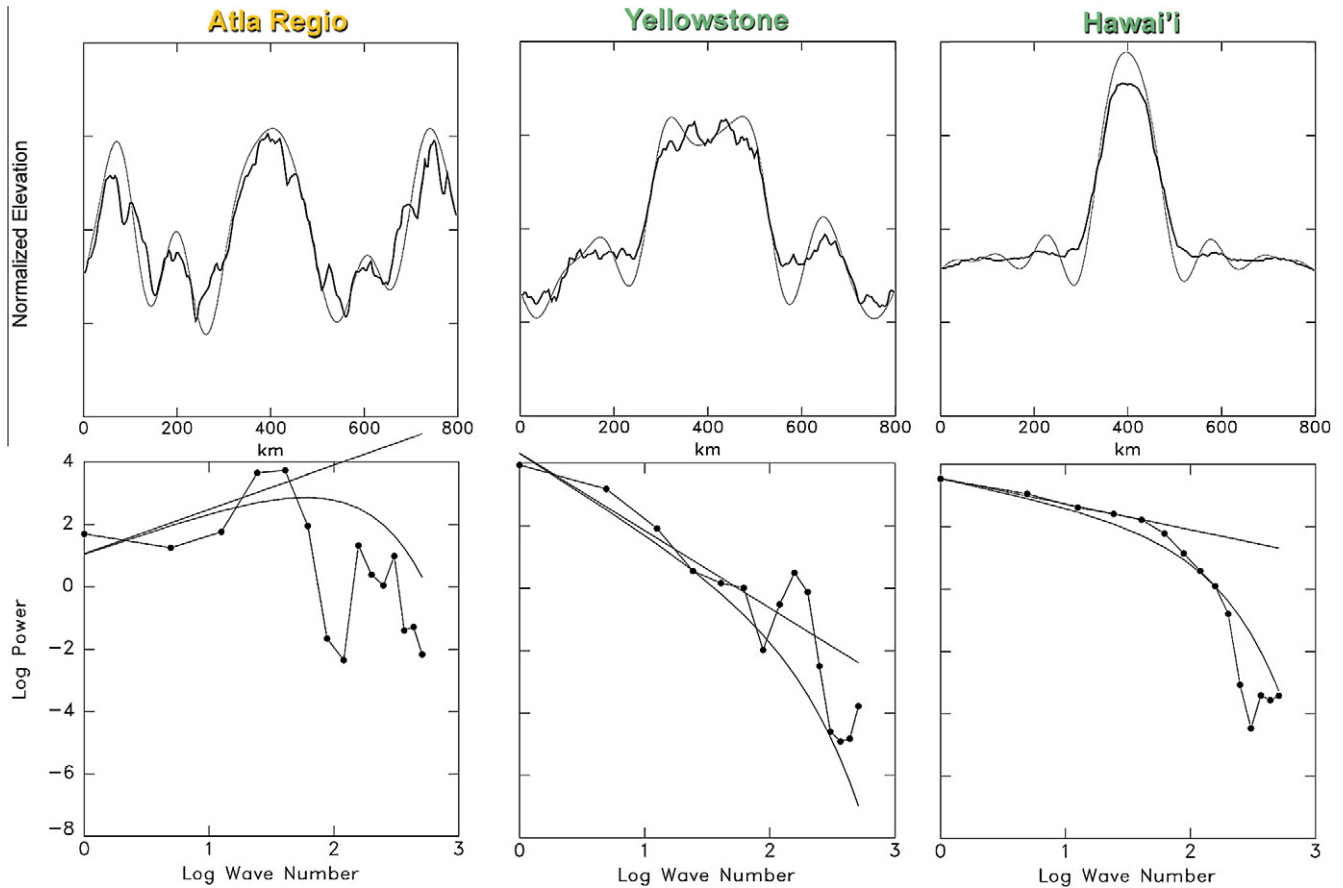
Fig. 9. Fourier analysis (top) and power spectra (bottom) for terrestrial (Yellowstone, Hawaii) and venusian uplifts (Atla Regio). Darker curve represents the average profile; the lighter curve, the Fourier fit using 15 components. Straight line shows a linear fit using only the first five wave numbers, and the curve represents the best fitting curve falling off with increasing wave number.

thick. Similarly, topographic profiles may also be sensitive to the local lithospheric thickness. Consideration of an expanded set of chasmata, ones in various settings, warrants further study. Principal component analysis may reveal further similarities.

Fourier analyses and the length-dependence of profile comparisons further characterizes the differences between topographic profiles for Venus and Earth. The Fourier decomposition of average topographic profiles shows that fast-spreading terrestrial ridges can be fit by just three components at the 98% level, whereas Venus' features require up to 15 components for the same level of fit. For Earth, shorter profiles correlate with each other better than do the longer profiles, while this trend is reversed for Venus. Additional analysis for a variety of profile lengths should be informative.

While this study does not definitively answer the question of whether or not lithospheric spreading is occurring on Venus, it does strongly suggest that if spreading is occurring it is happening at very slow rates. Comparisons of uplift features reaffirm ideas of a thick lithosphere for Venus, and of rifting as the dominant process for Atla and Beta regiones.

Topographic data are relatively easy to collect, and we have shown that they can provide valuable insight into some of the fundamental surface features and processes for our nearest terrestrial neighbor, Venus. As more data become available, it will be very interesting to expand the comparison to the hypsography of terrestrial and icy world.

Acknowledgments

Appendix A. Principal component analysis

The theory of real symmetric matrices and the fact that such matrices can be diagonalized by a rotation matrix (whose inverse is its transpose and whose columns are orthogonal vectors) is outlined very nicely in Press et al. (1992, Section 11) or any linear algebra book (e.g. Lay, 2006).

If we have a set of elevation profiles, $z_n(x_r)$, which are normalized so that their mean value is zero and have some defined standard deviation, then we can form a covariance matrix, c_{mn}

$$c_{mn} = \sum_x z_m(x) z_n(x)$$

This matrix can be diagonalized by means of a rotation matrix, v_{rs}, such that

$$\sum_n \sum_m v_{mr} c_{mn} v_{ns} = \lambda_r^2 \delta_{rs}$$

This can and usually is rewritten as an eigenvalue equation

$$\sum_n C_{mn} v_{ns} = \lambda_s^2 v_{ms}$$

since

$$\sum v_{mr} v_{ms} = \delta_{rs}$$

The matrix v_{ms} and the original height profiles $z_m(x)$ can be used to construct "principal components"

$$h_s(x) = \sum_m v_{ms} z_m(x)$$

The covariance matrix of these new profiles is diagonal, i.e. these profiles are uncorrelated and have some larger mean square values than others, which makes them more important than the others.

References

Adams, K.A., Jurdy, D.M., 2011. Pit distribution in the equatorial region of Titan. Planet. Space Sci., submitted for publication (Titan through time).

Basilevsky, A.T., Head, J.W., 2002. Venus: Timing and rates of geologic activity. Geology 30, 1015–1018.

Bleamaster, L.F., Hansen, V.L., 2004. Effects of crustal heterogeneity on the morphology of chasmata. Venus: J. Geophys. Res. 109 (E0). doi:10.1029/2003JE002193.

Courtillot, V., Davaille, A., Besse, J., Stock, J., 2003. Three distinct types of hotspots in the Earth's mantle. Earth Planet. Sci. Lett. 205, 295–308.

Dick, H.J.B., Lin, J., Schouten, H., 2003. An ultra-slow spreading class of oceanic ridge. Nature 426, 405–412.

Feder, J., 1988. Fractals. Plenum, New York, 283pp..

Ford, P.G., Pettengill, G.H., 1992. Venus topography and kilometer-scale slopes. J. Geophys. Res. 97, 13103–13114.

Foulger, G.R., Jurdy, D.M., 2007. Preface. In: Foulger, G.R., Jurdy, D.M. (Eds.), Plumes, Plates and Planetary Processes, Geological Society of America Special Paper #430, Containing 46 Papers and ~150 Discussion Pieces, 997pp.

Head, J.W., Hiesinger, H., Ivanov, M.A., Kreslavsky, M.A., Pratt, S., Thomson, B.J., 1999. Possible ancient oceans on Mars: Evidence from Mars orbiter laser altimeter data. Science 286, 2134–2137 (10.1126).

Huang, J., Turcotte, D.L., 1989. Fractal mapping of digitized images: Application to the topography of Arizona and comparisons with synthetic images. J. Geophys. Res. 94, 7491–7495.

Jurdy, D.M., Stefanick, M., 1999. Correlation of Venus surface features and geoid. Icarus 139, 93–99.

Jurdy, D.M., Stoddard, P.R., 2007. The coronae of Venus: Impact, plume or other origin. In: Foulger, G.R., Jurdy, D.M. (Eds.), Plates, Plumes and Planetary Processes. Geological Society of America Special Paper 430, pp. 859–878. Geological Society of America, Boulder Co, 997pp.

Kaula, W.M., Phillips, R.J., 1981. Quantitative tests for plate tectonics on Venus. Geophys. Res. Lett. 8, 1187–1190.

Kucinskas, A.B., Turcotte, D.L., Huang, J., Ford, P.G., 1992. Fractal analysis of Venus topography in Tinatin Planitia and Ovda Regio. J. Geophys. Res. 97, 13635–13641.

Lay, D.C., 2006. Linear Algebra and its Applications. Pearson, Addison-Wesley, New York, 492pp..

Lorenz, R.D., Tuttle, E.P., Stiles, B., Le Gall, A., Hayes, A., Aharonson, O., Wood, C.A., Stofan, E., Kirk, R., 2011. Hypsometry of Titan. Icarus, 699–706.

Matias, A., Jurdy, D.M., 2005. Impact craters as indicators of tectonic and volcanic activity in the Beta–Atla–Themis region, Venus. In: Foulger, G.R., Natland, J.H., Presnall, D.C., Anderson, D.L. (Eds.), Plates, Plumes, and Paradigms, Geological Society of America Special Paper 388, pp. 825–839. Geological Society of America, Boulder Co, 881pp.

NOAA, 1988. Data Announcement 88-MGG-02, Digital Relief of the Surface of the Earth, National Geophysical Data Center, Boulder, Colorado.

Parker, T.J., Gorsline, D.S., Saunders, R.S., Pieri, D.C., Schneeberger, D., 1993. Coastal geomorphology of the martian northern plains. J. Geophys. Res. 98, 11061–11078.

Parsons, B., 1981. The rates of plate creation and consumption. Geophys. J. Roy. Astron. Soc. 67, 437–448.

Press, W.H., Teukolsky, S.A., Vetterling, W.T., Flannery, B.P., 1992. Numerical Recipes in FORTRAN. Cambridge University Press, New York, 818pp..

Price, M., Suppe, J., 1995. Constraints on the resurfacing history of Venus from the hypsometry and distribution of tectonism, volcanism, and impact craters. Earth Moon Planets 71, 99–145.

Schaber, G.G., 1982. Venus: Limited extension and volcanism along zones of lithospheric weakness. Geophys. Res. Lett. 9, 499–502.

Smith, D.E., Zuber, M.T., 1996. The shape of Mars and the topographic signature of the hemispheric dichotomy. Science 271, 184–188. doi:10.1126/science.271.5246.184.

Stoddard, P.R., 1992. On the relation between transform fault resistance and plate motion. J. Geophys. Res. 97, 17637–17650.

Stoddard, P.R., Jurdy, D.M., 2005. Comparison of topographic profiles on Venus and Earth. Lunar Planet Sci. XXXVI. Abstract 2247.

Stofan, E.R., Smrekar, S.E., 2005. Large topographic rises, coronae, large flow fields, and large volcanoes on Venus: Evidence for mantle plumes? In: Foulger, G.R., Natland, J.H., Presnall, D.C., Anderson, D.L. (Eds.), Plates, Plumes, and Paradigms, Geological Society of America Special Paper 388, pp. 841–861. Geological Society of America, Boulder Co, 881pp.

Wegener, A., 1966. The origin of continents and oceans. In: J. Biram (Ed.), Trans. from the 1929 4th German. New York, Dover, 246pp.